Tetrathiafulvalene Derivatives as NLO-phores: Synthesis, Electrochemistry, Raman Spectroscopy, Theoretical Calculations, and NLO Properties of Novel TTF-Derived Donor-π-Acceptor Dyads

Mar González, José L. Segura, Carlos Seoane, and Nazario Martín*

Departamento de Química Orgánica, Facultad de Química, Universidad Complutense, E-28040 Madrid, Spain

Javier Garín* and Jesús Orduna

Departamento de Química Orgánica, ICMA, Universidad de Zaragoza-CSIC, E-50009 Zaragoza, Spain

Rafael Alcalá and Belén Villacampa

Departamento de Física de la Materia Condensada, ICMA, Universidad de Zaragoza, CSIC, E-50009 Zaragoza, Spain

Víctor Hernández and Juan T. López Navarrete*

Departamento de Química Física, Facultad de Ciencias, Universidad de Málaga, E-29071 Málaga, Spain

nazmar@eucmax.sim.ucm.es

Received July 16, 2001

Novel π-conjugated donor−acceptor chromophores, based on the strong electron-donating tetrathiafulvalene moiety and different electron-withdrawing acceptors, exhibit large second-order optical nonlinearities. The effect of increasing the length of the polyenic spacer and the influence of the nature of the acceptor moiety on the NLO properties have been studied by using the electric field-induced second-harmonic generation (EFISH) technique as well as by semiempirical and ab initio theoretical calculations. A charge-transfer band has been observed in the absorption spectra of these D-π-A compounds that undergoes an hypsochromic shift when increasing the number of vinylenic spacer units connecting both donor and acceptor moieties. The degree of the intramolecular charge transfer from the donor to the acceptor has also been analyzed by means of Raman spectroscopy.

Introduction

Donor (D)−acceptor (A) substituted organic molecules with large second-order nonlinear optical (NLO) properties have been the subject of considerable research efforts due to their potential applications in areas such as optical modulation, molecular switching, optical memory, and frequency doubling.[1,2] Although organic molecules are not as robust as inorganics, they have received a great deal of interest in the nonlinear optics field given that they offer many advantages over traditional inorganic crystals: (i) organic materials present high electronic susceptibility ($\chi^{(2)}$) through high molecular hyperpolarizability (β) and fast response time; (ii) they are cheaper to produce and (iii) easier to fabricate; (iv) they are compatible with existing semiconductor technology; and (v) their structures can be tailored in myriads of ways allowing to finely tune NLO properties for desired applications.

A key objective in the development of materials for nonlinear optical applications is to find highly active chromophores with large second-order polarizabilities β. The first hyperpolarizability and, hence, the second-order NLO response is related to an electronic intramolecular charge transfer (ICT) excitation between the ground and excited states of the molecule. Both theoretical and experimental studies have shown that large hyperpolarizabilities generally arise from a combination of a strong electron donor and acceptor positioned at opposite ends of a suitable conjugation path. Thus, a variety of donor−

(1) (a) *Nonlinear Optical Properties of Organic Molecules and Crystals*; Chemla, D. S., Zyss, J., Eds.; Academic Press: New York, 1987. (b) *Materials for Nonlinear Optics: Chemical Perspectives*; Marder, S. R., Sohn, J. E., Stucky, G. D., Eds; ACS Symposium Series; American Chemical Society: Washington, DC, 1991. (c) Optical Nonlinearities in Chemistry. *Chem. Rev.* **1994**, *94*(1). (d) Bosshard, C.; Sutter, K.; Pretre, P.; Hulliger, J.; Flörsheimer, M.; Kaatz, P.; Günter, P. *Organic Nonlinear Optical Materials*; Gordon & Breach: Basel, 1995. (e) *Polymers for Second-Order Nonlinear Optics*; Lindsay, G. A., Singer, K. D., Eds.; ACS Symposium Series Vol. 601; American Chemical Society: Washington, DC, 1995. (f) Kajzar, F.; Swalen, J. *Organic Thin Films for Waveguiding Nonlinear Optics*; Gordon & Breach: Amsterdam, 1996. (g) Miyata, S.; Sasabe, H. *Poled Polymers and Their Applications to SHG and EO Devices*; Gordon & Breach: Amsterdam, 1997. (h) Nalwa, H. S. *Nonlinear Optics of Organic Molecules and Polymers*; CRC Press: Boca Raton, 1997. (i) Kuzyk, M. G.; Singer, K. D.; Twieg, R. J. *J. Opt. Soc. Am. B. Opt. Phys.* **1998**, *15*, 254.

(2) (a) Marks, T. J.; Ratner, M. A. *Angew. Chem., Int. Ed. Engl.* **1995**, *34*, 155. (b) Denning, R. G. *J. Mater. Chem.* **1995**, *5*, 365. (c) Marder, S. R.; Kippelen, B.; Jen, A. K.-Y.; Peyghambarian, N. *Nature* **1997**, *388*, 845. (d) Wolff, J. J.; Wortmann, R. *J. Prakt. Chem.* **1998**, *340*, 99. (e) Cotter, D.; Manning, R. J.; Blow, K. J.; Ellis, A. D.; Kelly, A. E.; Nesset, D.; Phillips, I. D.; Poustie, A. J.; Rogers, D. C. *Science* **1999**, *286*, 1523. (f) Dalton, L. R.; Steier, W. H.; Robinson, B. H.; Zhang, C.; Ren, A.; Garner, S.; Chen, A.; Londergan, T.; Irwin, L.; Carlson, B.; Fifield, L.; Phelan, G.; Kincaid, G.; Amend, J.; Jen, A. *J. Mater. Chem.* **1999**, *9*, 1905.

10.1021/jo010717k CCC: $20.00
Published on Web 11/30/2001

acceptor organic molecules containing different acceptor units such as nitro,[3] nitrile,[4] sulfonyl,[5] polycyanovinyl,[6] 4-methylidene-3-phenylisoxazolone,[7] 4-methylidenedieth-ylthiobarbituric acid,[7] phosphonate,[8] 1,3-bis(dicyano-methyliden)indan,[9] 3-dicyanomethylen-2,3-dihydroben-zothiophen-2-yliden-1,1-dioxide,[10] pyridinium salts[11] or diazonium salts[12] and donor units such as dialkyl-amines,[13] alkoxyaryl groups,[14] ferrocene,[15] guanidyl,[16] phosphoranimidyl,[16] azulene[17] or the 1,3-dithiole ring[6a,18,19] have been previously reported (Chart 1).

In this context, we reported in 1997 the first NLO materials containing the TTF unit as the donor moiety in D-π-*A* systems.[20] Although TTF and its derivatives were originally prepared as strong electron-donor mol-ecules for the development of electrically conducting materials, during recent years they have shown new and

Chart 1

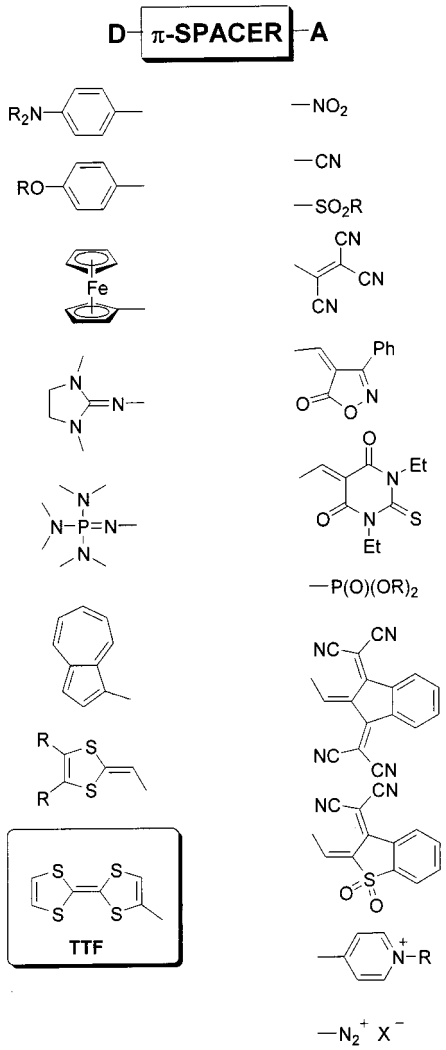

in some cases little exploited possibilities.[21] After our investigations have confirmed that TTF derivatives can display efficient NLO responses,[20,22] the combination of

(3) (a) Keshari, U.; Korna, S. P.; Prasad, N. P. *J. Phys. Chem.* **1993**, *97*, 3525. (b) Morley, J. O.; Hutchings, M. G.; Zyss, J.; Ledoux, I. *J. Chem. Soc., Perkin Trans. 2* **1997**, 1139.

(4) Müller, T. J. J.; Robert, J. P.; Schmälzlin, E.; Bräuchle, Meerholz, K. *Org. Lett.* **2000**, *2*, 2419.

(5) (a) Chou, S.-S.; Hsu, G.-T.; Lin, H.-C. *Tetrahedron Lett.* **1999**, *40*, 2157. (b) Chou, S.-S. P.; Sun, D. J.; Lin, H.-C.; Yang, P.-K. *Chem. Commun.* **1996**, 1045.

(6) (a) De Lucas, A. I.; Martín, N.; Sánchez, L.; Seoane, C.; Garín, J.; Orduna, J.; Alcalá, R.; Villacampa, B. *Tetrahedron Lett.* **1997**, *38*, 6107. (b) Katz, H. E.; Singer, K. D.; Sohn, J. E.; Dirk, C. W.; King, L. A.; Gordon, H. M. *J. Am. Chem. Soc.* **1987**, *109*, 6561.

(7) (a) Bedowrth, P. V.; Cai, Y.; Jen, A.; Marder, S. R. *J. Org. Chem.* **1996**, *61*, 2242. (b) Cho, B. R.; Son, N. K.; Lee, S. J.; Kang, T. I.; Han, M. S.; Jeon, S. J.; Song, N. W.; Kim, D. *Tetrahedron Lett.* **1998**, *39*, 3167.

(8) Belfield, K.; Chinna, C.; Schafer, K. *Tetrahedron Lett.* **1997**, *38*, 6131.

(9) Sun, S.; Zhang, C.; Dalton, L.; Garner, S.; Chen, A.; Steier, W. *Chem. Mater.* **1996**, *8*, 2539.

(10) Ahlheim, M.; Barzoukas, M.; Bedworth, P.; Blanchard-Desce, M.; Fort, A.; Hu, Z.; Marder, S.; Perry, J.; Runser, C.; Staehelin, M.; Zysset, B. *Science* **1996**, *271*, 335.

(11) (a) Marder, S. R.; Perry, J. W.; Yakymyshyn, C. P. *Chem. Mater.* **1994**, *6*, 1137. (b) Coradin, T.; Nakatani, K.; Ledoux, I.; Zyss, J.; Clément, R. *J. Mater. Chem.* **1997**, *7*, 853.

(12) Kang, S. H.; Jeon, Y.-M.; Kim, K.; Houbrechts, S.; Hendrickx, E.; Persoons, A. *J. Chem. Soc., Chem. Commun.* **1995**, 635.

(13) (a) Jen, A. K.-Y.; Rao, V. P.; Wpong, K. Y.; Drost, K. J. *J. Chem. Soc., Chem. Commun.* **1993**, 90. (b) Shu, C.-F.; Tsai, W. J.; Chen, J.-Y.; Jen, A. K.-Y.; Zhang, Y.; Chen, T.-A. *Chem. Commun.* **1996**, 2279.

(14) Li, F.-Y.; Zheng, J.; Jin, L.-P.; Zhao, X.-S.; Liu, T.-T.; Guo, J.-Q. *J. Mater. Chem.* **2000**, *10*, 1287.

(15) (a) Barlow, S.; Bunting, H. E.; Ringham, C.; Green, J. C.; Bublitz, G. U.; Boxer, S. G.; Perry, J. W.; Marder, S. R. *J. Am. Chem. Soc.* **1999**, *121*, 3715. (b) Iftime, G.; Balavoine, G. G. A.; Daran, J.-C.; Lacroix, P. G.; Manoury, E. *C. R. Acad. Sci. Paris, Sér. Iic, Chim.* **2000**, *3*, 139. (c) Barlow, S.; Marder, S. *Chem. Commun.* **2000**, 1555.

(16) Boldt, P.; Eisenträger, T.; Glania, C.; Göldenitz, J.; Krämer, P.; Matschiner, R.; Rase, J.; Schwesinger, R.; Wichern, J.; Wortmann, R. *Adv. Mater.* **1996**, *8*, 672.

(17) (a) Asato, A. E.; Liu, R. S. H.; Rao, V. P.; Cai, Y. M. *Tetrahedron Lett.* **1996**, *37*, 419. (b) Iftime, G.; Lacroix, P. G.; Nakatani, K.; Razus, A. C. *Tetrahedron Lett.* **1998**, *39*, 6853. (c) Lacroix, P. G.; Malfant, I.; Iftime, G.; Razus, A. C.; Nakatani, K.; Delaire, J. A. *Chem. Eur. J.* **2000**, *6*, 2599.

(18) (a) Jen, A. K.-Y.; Rao, V. P.; Drost, K. J.; Wong, K. Y.; Cava, M. P. *J. Chem. Soc., Chem. Commun.* **1994**, 2057. (b) Blanchard-Desce, M.; Ledoux, I.; Lehn, J. M.; Malthete, J.; Zyss, J. *J. Chem. Soc., Chem. Commun.* **1988**, 737. (c) Meyers, F.; Bredás, J. L.; Zyss, J. *J. Am. Chem. Soc.* **1992**, *114*, 2914. (d) Inoue, S.; Mikami, S.; Aso, Y.; Otsubo, T.; Wada, T.; Sasabe, H. *Synth. Met.* **1997**, *84*, 395. (e) Inoue, S.; Aso, Y.; Otsubo, T. *Chem. Commun.* **1997**, 1105. (f) Moore, A. J.; Bryce, M. R.; Batsanov, A. S.; Green, A.; Howard, J. A. K.; McKervey, M. A.; McGuigan, P.; Ledoux, I.; Ortí, E.; Viruela, R.; Tarbit, B. *J. Mater. Chem.* **1998**, *8*, 1173. (g) Nguyen, T. T.; Sallé, M.; Delaunay, J.; Riou, A.; Richomme, P.; Raimundo, J. M.; Gorgues, A.; Ledoux, I.; Dhenaut, C.; Zyss, J.; Orduna, J.; Garín, J. *J. Mater. Chem.* **1998**, *8*, 1185.

(19) Batsanov, A. S.; Bryce, M. R.; Coffin, M. A.; Green, A.; Hester, R. E.; Howard, J. A. K.; Lednev, I. K.; Martín, N.; Moore, A. J.; Moore, J. N.; Ortí, E.; Sánchez, L.; Savirón, M.; Viruela, P. M.; Viruela, R.; Ye, T. *Chem. Eur. J.* **1998**, *4*, 2580.

(20) (a) Andreu, R.; de Lucas, A. I.; Garín, J.; Martín, N.; Orduna, J.; Sánchez, L.; Seoane, C. *Synth. Met.* **1997**, *86*, 1817. (b) De Lucas, A. I.; Martín, N.; Sánchez, L.; Seoane, C.; Andreu, R.; Garín, J.; Orduna, J.; Alcalá, R.; Villacampa, B. *Tetrahedron* **1998**, *54*, 4655.

(21) For some recent reviews on TTF, see: (a) Bryce, M. R. *Chem. Soc. Rev.* **1991**, *20*, 355. (b) Khodorkovsky, V.; Becker, J. Y. In *Organic Conductors*; Farges, J.-P., Ed.; Dekker: New York, 1994; Chapter 3. (c) Bryce, M. R. *J. Mater. Chem.* **1995**, *5*, 1481. (d) Schukat, G.; Richter, A. M.; Fanghänel, E. *Sulfur Rep.* **1987**, *7*, 155. (e) Schukat, G.; Fanghänel, E. *Sulfur Rep.* **1993**, *14*, 245. (f) Schukat, G.; Fanghänel, E. *Sulfur Rep.* **1996**, *18*, 1. (g) Garín, J. *Adv. Heterocycl. Chem.* **1995**, *62*, 249. (h) Simonsen, K. B.; Svenstrup, N.; Lau, J.; Simonsen, O.; Mørk, P.; Kristensen, G. J.; Becher, J. *Synthesis* **1996**, 407. (i) Otsubo, T.; Aso, Y.; Takimiya, K. *Adv. Mater.* **1996**, *8*, 203. (j) Adam, M.; Müllen, K. *Adv. Mater.* **1994**, *6*, 439. (k) Becher, J.; Lau, J.; Mørk, P. In *Electronic Materials: The Oligomer Approach*; Müllen, K., Wegner, G., Eds.; Wiley-VCH: New York, 1998; pp 198−233. (l) Bryce, M. R.; Davenport, W.; Goldenberg, L. M.; Wang, C. *Chem. Commun.* **1998**, 945. (m) Jørgensen, T.; Hansen, T. K.; Becher, J. *Chem. Soc. Rev.* **1994**, 41. (n) Simonsen, K. B.; Becher, J. *Synlett* **1997**, 1211. (o) Nielsen, M. B.; Becher, J. *Liebigs Ann./Recueil* **1997**, 2177. (p) Coronado, E.; Gómez-García, C. J. *Chem. Rev.* **1998**, *98*, 273. (q) Roncali, J. *J. Mater. Chem.* **1997**, *7*, 2307. (r) Day, P.; Kurmoo, M. *J. Mater. Chem.* **1997**, *8*, 1291. (s) Bryce, M. R. *Adv. Mater.* **1999**, *11*, 11. (t) Nielsen, M. B.; Lomholt, C.; Becher, J. *Chem. Soc. Rev.* **2000**, *29*, 153. (u) Bryce, M. R. *J. Mater. Chem.* **2000**, *10*, 589. Segura, J. L.; Martín, N. *Angew. Chem., Int. Ed.* **2001**, *40*, 1372.

(22) A previous communication on the synthesis of compounds **2a**−**c** and **4** has been reported: (a) Garín, J.; Orduna, J.; Rupérez, J. I.; Alcalá, R.; Villacampa, B.; Sánchez, C.; Martín, N.; Segura, J. L.; González, M. *Tetrahedron Lett.* **1998**, *39*, 3577. (b) González, M.; Martín, N.; Segura, J. L.; Seoane, C.; Garín, J.; Orduna, J.; Alcalá, R.; Sánchez, C.; Villacampa, B. *Tetrahedron Lett.* **1999**, *40*, 8599. (c) For a recent review, see: Garín, J.; Orduna, J.; Andreu, R. *Recent Res. Devel. Org. Chem.* **2001**, *5*, 77.

Chart 2

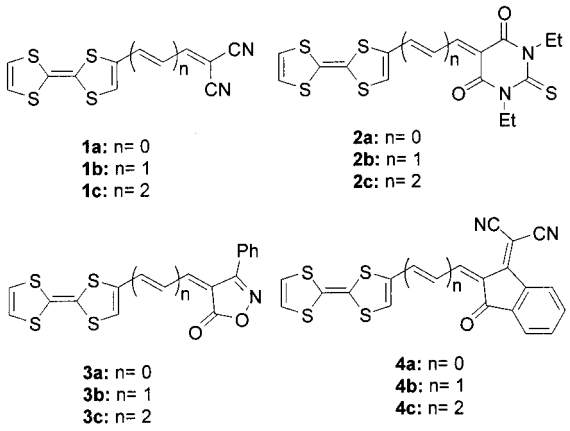

this property with the redox ability of TTF as external stimuli can be envisaged as a promising strategy for the molecular engineering of switchable NLO materials.[23] Thus, in this paper, we present the synthesis of a series of TTF-containing molecules in which the acceptor part as well as the length of the π-spacer have been systematically modified in order to optimize second-order NLO responses. As the acceptor counterpart we have chosen different moieties that have been successfully used in the synthesis of efficient NLO-phores. To gain an understanding on the observed NLO properties of the novel TTF-based D-π-A systems as well as on their geometrical and electronic properties, theoretical calculations at the semiempirical (PM3) and ab initio level have been carried out. The electronic and Raman spectra complement this study.

Results and Discussion

Synthesis. The synthesis of TTF-π-*A* derivatives (**1**−**4**, Chart 2) has been carried out by reaction of appropriately functionalized acceptor moieties with formyl-TTF and its vinylogues. Lithiation of tetrathiafulvalenes constitutes the most significant route for the preparation of TTF derivatives given that the metalated species formed give rise to a wealth of new derivatives.[21g,24] The synthesis of formyl-TTF (**5a**) was first reported by Green[24] by reaction of monolithio-TTF with dimethylformamide. Afterward, Garín, Bryce, and co-workers thoroughly investigated this reaction with a variety of formylating reagents in order to increase the yields and optimize the preparation of formyl-TTF (**5a**).[25] Subsequent Wittig reaction of formyl-TTF with phosphorane **6** leads to the formyl-TTF vinylogue **5b** with an overall yield of 51% starting from TTF (Scheme 1). To the best of our knowledge, the preparation of higher vinylogues by following this or any other synthetic route has not yet been reported.

To systematically increase the length of the polyenic spacer between the donor and acceptor units in these D-π-A systems, the synthesis of longer vinylogues of **5a** were required. Thus, we have recently reported in a preliminary communication an alternative one-pot synthesis of **5b** as well as the synthesis of the higher vinylogue **5c** (Scheme 1).[26]

The key step in the general reaction scheme involves the reaction of monolithio-TTF (generated from TTF and lithium diisopropylamide) with the commercially available *N*,*N*-dimethylaminoacrolein (**7**) to yield **5b** and with 5-(*N*,*N*-diethylamino)-4-pentadienal (**8**)[27] to obtain **5c** by following Jutz's procedure,[28] which has been recently extended to several organolithium systems by Friendli, Yang, and Marder.[29] All-trans vinylogue amides were used in all cases as starting materials, and only all-trans vinylogues were obtained according to the coupling constants observed in the ^{1}H NMR spectra.

As previously stated, we reported the synthesis of the first NLO materials containing the TTF unit as the donor moiety and dicyanomethylene as the acceptor group (**1a**,**b**).[20] Now we have extended these series to **1c** by incorporating another vinylene unit between the donor and acceptor moieties. This compound was obtained in 60% yield from **5c** by Knoevenagel condensation with malononitrile under basic conditions (Scheme 1). Due to the presence of the conjugated nitrile group in **1c**, bands at 2230 ad 2219 cm^{-1} can be observed in the FT-IR spectra and two signals at ca. 115 ppm are present in the ^{13}C NMR spectra.

As noted above, following these first examples of TTF-containing D-π-A systems, we have extended these series to new acceptor moieties. Marder has proposed a model that correlates the molecular hyperpolarizability value β with the degree of charge separation in the ground state.[30] This research group has shown how stilbenes or diphenylpolyenes endowed with donor and acceptor groups exhibit a loss of aromaticity in these moieties, which produces a deficient contribution of resonance forms with charge separation. To solve this problem, new acceptor moieties have been designed having a topology that allows a gain in aromaticity in the charge-separated state. These acceptor groups, frequently used in the design of D−A systems for NLO, are the 3-phenyl-5-isoxazolone and the *N*,*N*′-diethylthiobarbituric acid.[7] Thus, we have chosen these groups to combine them with the TTF moiety in order to extend the study of the NLO properties of TTF derivatives. The syntheses of these new series of compounds (**2a**−**c**, **3a**−**c**) have been carried out by Knoevenagel condensation between formyl-TTFs (**5a**−**c**) and the corresponding *N*,*N*′-diethylthiobarbituric acid (**9**) and 3-phenyl-5-isoxazolone (**10**), respectively. Best results have been obtained by simply refluxing stiochiometric amounts of both reagents in ethanol, while the mixture was protected from light and oxygen (Scheme 2). The attempted use of different catalysts, such as ethylenediammonium diacetate or piperidine, invariably led to decomposition products.

Attempts to obtain compound **3a** invariably led to a mixture of decomposition products while derivatives **3b**,**c** have been obtained in 72 and 69% yield, respectively. The structure of these compounds has been confirmed by their spectroscopic and analytical data. The signals corresponding to the ethylenic protons in the ^{1}H NMR spectra

(23) Coe, B. J. *Chem Eur. J.* **1999**, *5*, 2464.
(24) Green, D. C. *J. Org. Chem.* **1979**, *44*, 1476.
(25) Garín, J.; Orduna, J.; Uriel, S.; Moore, A. J.; Bryce, M. R.; Wegener, S.; Yufit, D. S.; Howard, J. A. K. *Synthesis*, **1994**, 489.
(26) González, M.; Martín, N.; Segura, J. L.; Garín, J.; Orduna, J. *Tetrahedron Lett.* **1998**, *39*, 3269.
(27) Becher, J. *Synthesis* **1980**, 589.
(28) Jutz, C. *Chem. Ber.* **1958**, *91*, 1867.
(29) Friendli, A. C.; Yang, E.; Marder, S. R. *Tetrahedron* **1997**, *53*, 2717 (*Corrigendum* **1997**, *53*, 6233).
(30) (a) Marder, S.; Beratan, D. *Science* **1991**, *252*, 103. (b) Meyers, F.; Marder, S.; Pierce, B.; Brédas, J. L. *J. Am. Chem. Soc.* **1994**, *116*, 10703.

Scheme 1

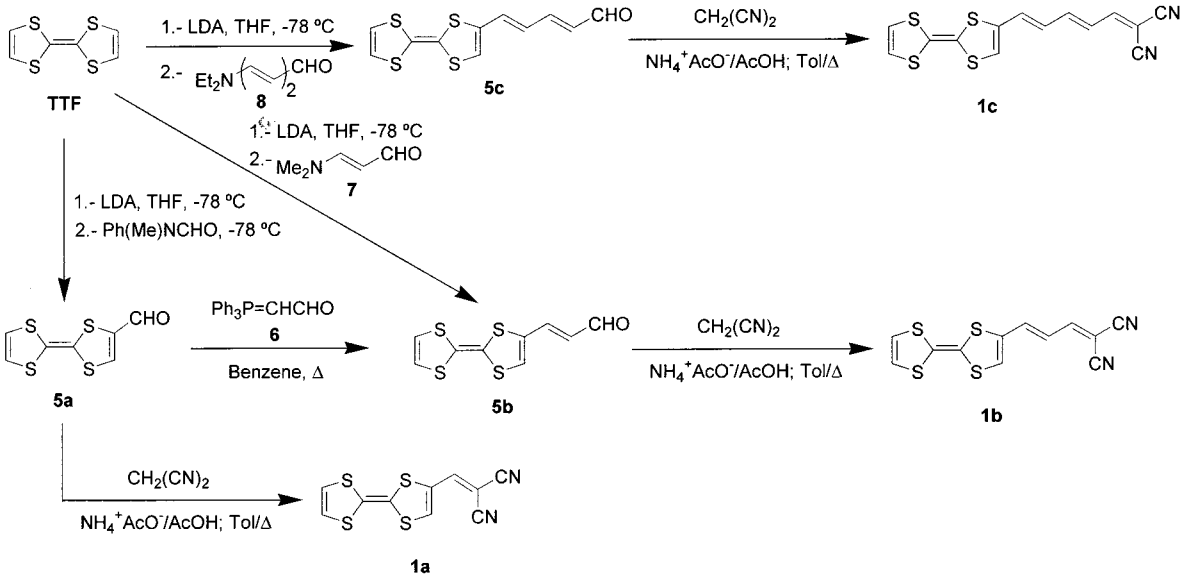

Scheme 2

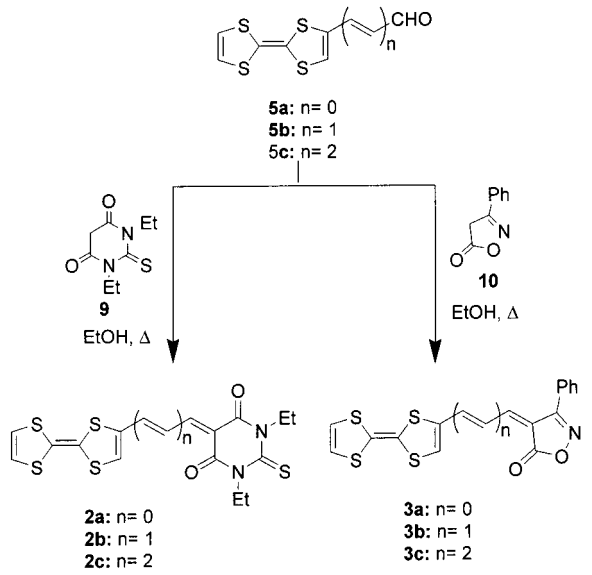

Scheme 3

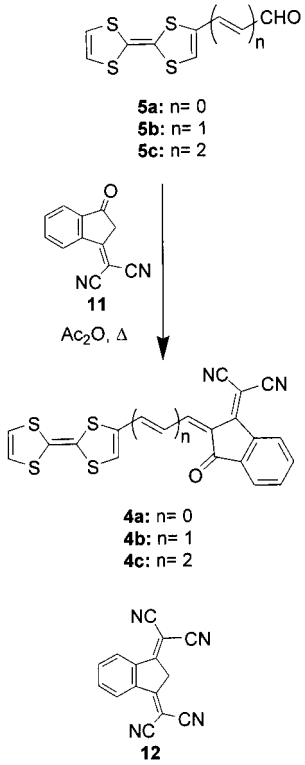

with $J = 13-15$ Hz indicate an all-trans configuration for the double bonds.

Other acceptor groups that have been successfully used for the synthesis of effective NLO materials are 3-(dicyanomethylen)indan-1-one (**11**) and 1,3-bis(dicyanomethylen)indan (**12**).[9] Thus, we have prepared compounds **4a**−**c** by refluxing stoichiometric amounts of both formyl-TTFs (**5a**−**c**) and 3-dicyanovinylindan-1-one (**11**) in acetic anhydride while the mixture was protected from light and oxygen (Scheme 3).

Derivatives **4a**−**c** were obtained as stable crystalline solids in moderate yields (45−52%). Their structure were confirmed by the spectroscopic and analytical data. Their FT-IR spectra exhibit bands at 2215 and 1700 cm^{-1} corresponding to the nitrile and carbonyl groups repectively. Interestingly, when a similar reaction was carried out using 1,3-bis(dicyanomethylene)indan as the acceptor moiety, highly insoluble dark materials were obtained. As a consequence of the strong donor ability of the TTF moiety and the strong acceptor character of the 1,3-bis(dicyanomethylene)indan system, formation of a charge-transfer complex in solution between the two molecules has to be taken into consideration. In fact, Batsanov et al. have reported that TTF and 1,3-bis(dicyanomethylene)indan form a 1:1 complex exhibiting semiconducting properties.[31] This fact strongly suggests that after combination of the TTF derivative with the tetracyano derivative of the indandione, a concurrence between the two reaction takes place, and the faster electron transfer process yields mainly the corresponding charge-transfer complexes.

Electrochemistry. The electrochemical properties of the new TTF-based NLO chromophores **1**−**4** have been

(31) Batsanov, A. S.; Bryce, M. R.; Davies, S. R.; Howard, J. A. K.; Whitehead, R.; Tanner, B. K. *J. Chem. Soc., Perkin Trans. 2* **1993**, 313.

Table 1. Redox Potentials for Compounds 1−4

compd	$E^1_{1/2,ox}$[a]	$E^2_{1/2,ox}$[a]	E^1_{red}[a]
1a	0.63	0.87	−0.89
1b	0.54	0.84	−0.87
1c	0.50	0.83	−0.87
2a	0.60	0.97	−0.63
2b	0.60	1.00	−0.57
2c	0.56	0.90	−0.52
3b	0.53	0.86	−0.88
3c	0.49	0.83	−0.91
4a	0.46	0.75	−0.96
4b	0.47	0.75	−0.96
4c	0.45	0.75	−0.97
TTF	0.37	0.73	−

[a] In volts vs SCE; CH_2Cl_2 as solvent, $Bu_4N^+ClO_4^-$ 0.1 M; 200 mV/s.

Table 2. Experimental $\mu\beta$ Values and Lowest Energy Absorption Bands for Compounds 1−4

compd	$\mu\beta_{exp}$[a]	$\mu\beta_{0exp}$[a]	λ_{max} (nm, in CH_2Cl_2)
1a			624
1b	470[b]	234[b]	618
1c	630[b]	320[b]	608
2a	480[c]	180[c]	718
2b	760[c]	347[c]	672
2c	960[c]	455[c]	648
3b	625[d]	295[d]	658
3c	1200[d]	611[d]	630
4b	700[d]	259[d]	726
4c	1350[d]	570[d]	690

[a] All $\mu\beta$ values in (10^{-48} esu). [b] Measured in chloroform at 1907 nm. [c] Measured in DMSO at 1907 nm. [d] Measured in dichloromethane at 1907 nm.

studied by cyclic voltammetry at room temperature in dichloromethane solutions, using glassy carbon as the working electrode, SCE as reference, and tetra-*n*-butylammonium perchlorate as the supporting electrolyte. The corresponding data are collected in Table 1 along with the redox potentials of the unsubstituted tetrathiafulvalene (TTF) used as reference.

All the voltammograms show two reversible one-electron oxidation waves corresponding to the TTF moiety, and one irreversible reduction wave, corresponding to the acceptor moiety. In all cases the oxidation potential values are shifted toward more positive values in comparison with unsubstituted TTF measured under the same experimental conditions, which is consistent with an increase in the oxidation potential produced by the presence of the acceptor moieties. The general trend is that this shift is bigger as the length of the spacer decreases indicating a stronger interaction between the donor and acceptor groups when they are closer.

Concerning the cathodic region of these voltammograms, the diethylthiobarbituric acid moiety shows the best electron acceptor properties, whereas derivatives **1**, **3**, and **4** present similar reduction potentials.

UV−vis, IR, and Raman Spectroscopy. The lowest energy absorption bands in electronic spectra observed for compounds **1**−**4** are given in Table 2. These bands (Figure 1) can be assigned to an intramolecular charge transfer (ICT) process and are subject to two general trends: (i) a red shift of the lowest energy absorption band is observed when increasing the acceptor ability of the acceptor moiety. The more red-shifted values of λ_{max} for derivatives **4** in comparison with that of derivatives **2** are an exception to this rule. (ii) The ICT band upshifts when the length of the oligoenic spacer is increased. This fact suggests that the extension of the charge transfer is

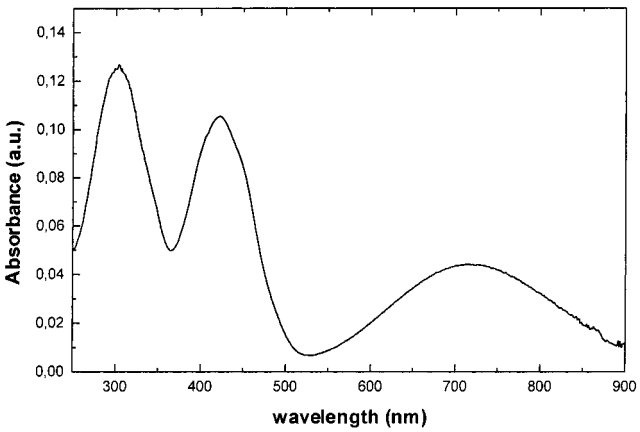

Figure 1. UV−vis spectrum of compound **4b**.

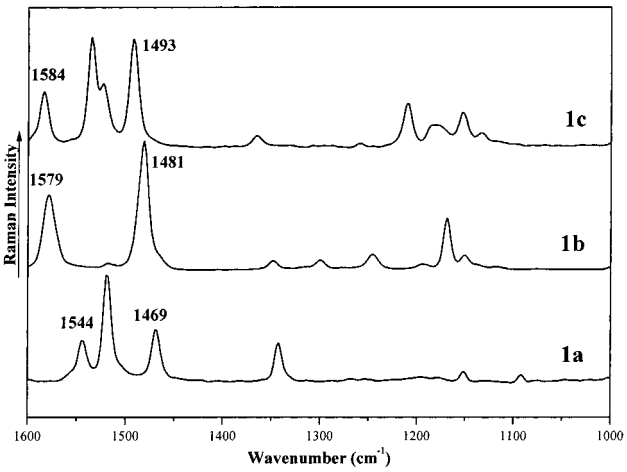

Figure 2. FT-Raman spectra of compounds **1a**−**c** in the 1600−1000 cm^{-1} Raman shift region.

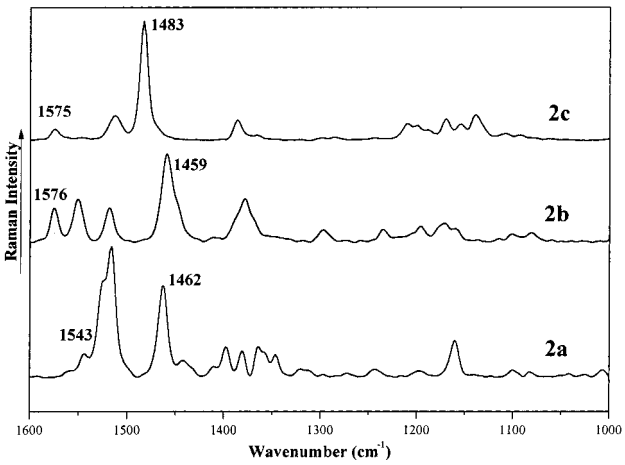

Figure 3. FT-Raman spectra of compounds **2a**−**c** in the 1600−1000 cm^{-1} Raman shift region.

reduced due to the inclusion of extra vinylenic double bonds in the spacer unit.

To analyze these experimental observations, we have carried out an IR and Raman spectroscopy study on these systems.

The Raman spectra of compounds **1a**−**c** and **2a**−**c** in the 1600−1000 cm^{-1} Raman shift region are shown in Figures 2 and 3, respectively. In view of the B3LYP[32]/6-31G**[33] vibrational eigenvectors plotted in Figure 4, the

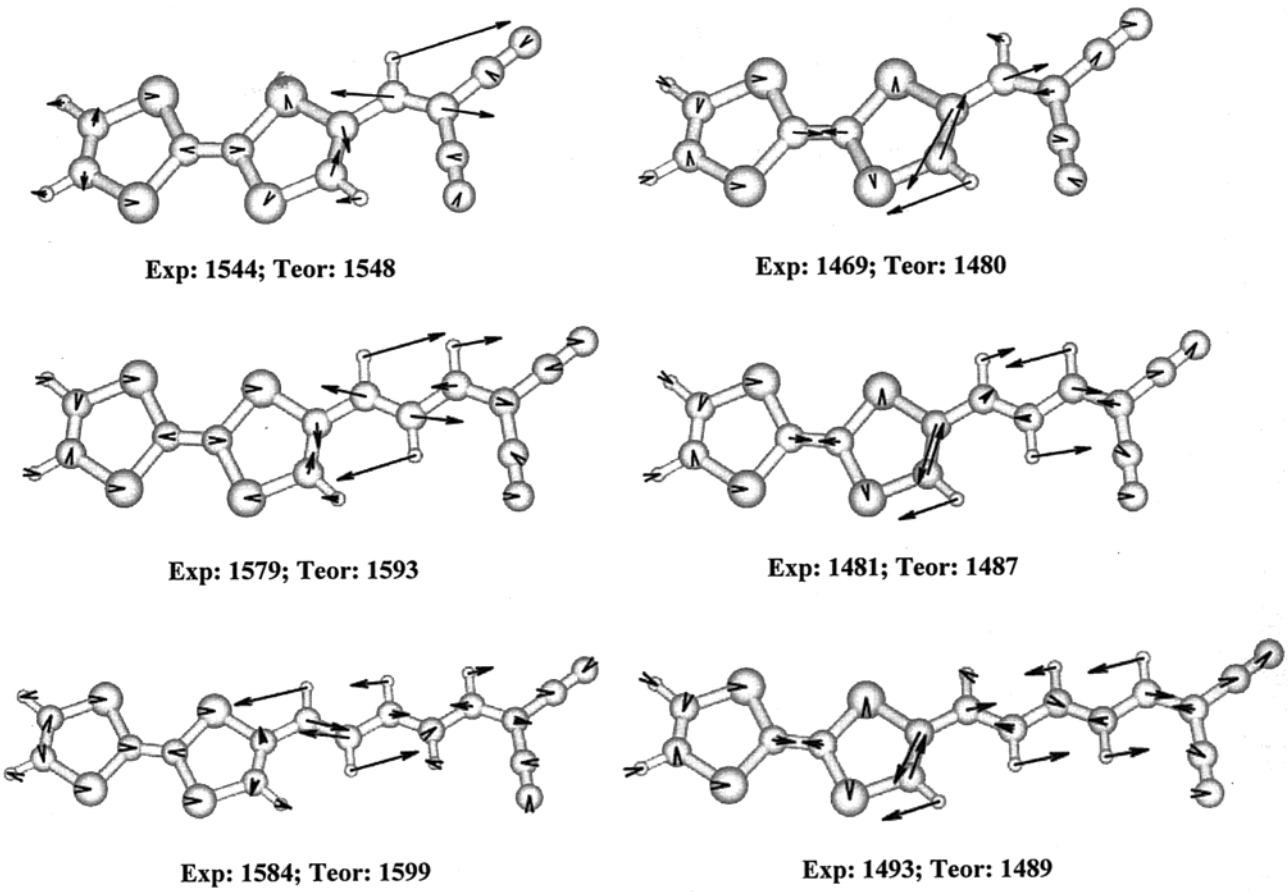

Figure 4. Schematic B3LYP/6-31G** atomic vibrational displacements associated with some of the most intense Raman lines of compounds **1a**−**c**.

Raman line around 1585−1540 cm^{-1} can be assigned to a ν(C═C) stretching mode of the vinylenic spacer coupled to some extent with a ν_s(C═C) stretching of the TTF donor unit, whereas the line near 1495−1470 cm^{-1} arises from a ν(C═C) stretching vibration mainly located on the TTF group, which extends toward the vinylenic spacer.

The two Raman lines undergo an upshift with increasing length of the π-spacer: 1544 and 1469 cm^{-1} (**1a**), 1579 and 1481 cm^{-1} (**1b**), and 1584 and 1493 cm^{-1} (**1c**) for the series of the dicyanomethylene acceptor group and 1543 and 1462 cm^{-1} (**2a**), 1576 and 1459 cm^{-1} (**2b**), and 1575 and 1483 cm^{-1} (**2c**) for the series of the *N*,*N*′-diethylthiobarbituric acid acceptor group.

Matsuzaki et al. have reported a Raman study of some mixed-valent and charge-transfer salts of TTF to determine either the formal charge or the degree of charge transfer, ρ, of the molecule or ion that forms the one-dimensional stack.[34−36] The plot of the Raman frequencies of the TTF salts vs ρ gives a straight line, and the formal charges of TTF estimated from the empirical relation agree well with those obtained from neutron and X-ray scatterings. The so-called ν_3 mode of TTF (associated to the stretching vibration of the central C═C bond) is measured at 1516 cm^{-1} in the neutral molecule ($\rho = 0$) and at 1420 cm^{-1} in the monocation ($\rho = 1$), and it shows the largest frequency shift with increasing ρ (ca. 100 cm^{-1}), thus giving the most reliable estimation of the formal charge or degree of charge transfer.

The ν_3 mode of the TTF moiety correlates with the Raman line near 1495−1470 cm^{-1} of our NLO chromophores. Under the assumption of general applicability of the linear relation ν_3 vs ρ proposed by these authors, the degree of intramolecular charge transfer can be estimated to be approximately 0.48 (**1a**), 0.37 (**1b**), and 0.25 (**1c**) for the series of the dicyanomethylene acceptor group and 0.57 (**2a**), 0.59 (**2b**), and 0.35 (**2c**) for the series of the *N*,*N*′-diethylthiobarbituric acid acceptor group. Thus, the values of ρ are found to be larger for the **2a**−**c** than for the **1a**−**c** compounds. These Raman results are in full agreement with the better electron acceptor properties of the diethylthiobarbituric acid as compared with the dicyanomethylene group. This Raman spectroscopy study reveals that of the six NLO-phores studied, **2b** displays the more effective intramolecular charge transfer. The increasing weight of the zwitterionic canonical structure (where an electron is fully transferred from the donor to the acceptor) in the stabilization of the electronic ground state could justify the high positive $E^1_{1/2,ox}$ and $E^2_{1/2,ox}$ values of **2b** (see Table 1).

In accordance with the trend of variation of the oxidation potentials on the chemical structure of these TTF-based NLO-phores, we observe that the Raman ν_3 mode of the TTF moiety upshifts in frequency as the

(32) Becke, A. D. *J. Chem. Phys.* **1993**, *98*, 5648.
(33) Francl, M. M.; Pietro, W. J.; Hehre, W. J.; Binkley, J. S.; Gordon, M. S.; Defrees, D. J.; Pople, J. A. *J. Chem. Phys.* **1982**, *77*, 3654.
(34) Matsuzaki, S.; Moriyama, T.; Toyoda, K. *Solid State Commun.* **1980**, *34*, 857.
(35) Matsuzaki, S.; Onomichi, M.; Tomura, H.; Yoshida, S.; Toyoda, K. *Mol. Cryst. Liq. Cryst.* **1985**, *120*, 93.
(36) Del Zoppo, M.; Castiglioni, C.; Zuliani, P. In *Handbook of Conductive Polymers, 2*; Skotheim, T. A., Elsembaumer, R. L., Reynolds, J., Eds.; Marcel Dekker: New York, 1998.

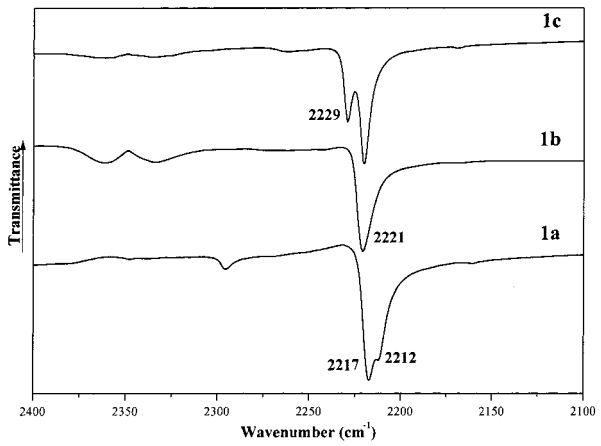

Figure 5. Infrared absorptions due to the CN end groups of compounds **1a**−**c**.

length of the π-bridge becomes longer, thus suggesting that the intramolecular charge transfer is less effective with increasing number of vinylenic units in the π-spacer.

The presence in push−pull molecules of a highly delocalized π-system gives rise to Raman spectra of a rather simple appearance: usually two to four lines with overwhelmingly strong activity dominate the whole spectrum. On the other hand, the electron-acceptor group withdraws electronic charge from the donor through the conjugated spacer, giving rise to a relevant molecular dipole moment roughly coincident with the chain axis of the molecule. For this reason, the shorter the chain length the stronger the bond polarization and more efficient the activation in the IR of the normal modes associated to the intramolecular charge transfer. On the contrary, the intensities of the few Raman bands experimentally observed continuously increase as the length of the spacer becomes longer, due to the increasing polarizability of the π-conjugated skeleton.

It has already been suggested the existence of a critical chain length in the class of the push−pull polyenes shown above in which the interaction between donor and acceptor groups is inhibited.[36,37] For chains with a length longer than the critical value, the bond polarization is confined within a few bonds close to the polar end groups, whereas the bonds in the middle of the π-bridge are practically apolar and still keep a strongly alternating polyene-like structure.

We observe that the frequencies of the infrared absorption bands due to the ν(C≡N) stretching modes also increase with increasing the length of the π-spacer: 2212 and 2217 cm^{-1} (**1a**), 2221 cm^{-1} (**1b**), and 2220 and 2229 cm^{-1} (**1c**) (see Figure 5). This finding has a straightforward explanation: as the chain length of the spacer becomes shorter (and more electronic charge is transferred from the donor to the acceptor end groups), the loss of triple bond character of the cyano groups (since the C≡N groups enter in the resonant stabilization of the zwitterionic form of the molecule) is more pronounced.

It has been suggested[38] on the basis of a one-dimensional model for the class of disubstituted D-π-A molecules, that the intramolecular charge transfer, Δq, from the donor to the acceptor end groups goes down roughly as $1/L$ (where L is the molecular length) and that the corresponding $L\Delta q$ contribution to the total dipole moment vary relatively slowly with length along a given series of chromophores with the same pair of donor and acceptor. The length dependence of β for such molecules is dominated by that of γ/α of the corresponding unsubstituted π-conjugated bridge (where γ and α are the third-order and linear polarizabilities, respectively) or roughly quadratic (L^2) as found experimentally (since $\alpha \approx L^3$ and $\gamma \approx L^5$).

It has also been hypothesized[39] that the ground-state polarization and bond length alternation (BLA) (i.e., the difference between average length of carbon−carbon double and single bonds in a polyenic chain) are useful parameters to consider when establishing structure−property relationships for NLO molecules. BLA varies from negative values for the neutral polyene structure, through zero for the polar cyanine-like structure, to positive values for the highly polar zwitterionic polyene structure. Also, as BLA changes from negative to positive values, the ground-state dipole moment, μ, increases, and at the same time, β initially increases, reaches a maximum, and begins to decrease, crossing through zero at BLA = 0 Å, and ultimately becomes negative when BLA is positive. This dependence of β on the ground-state polarization and BLA for a series of donor−acceptor disubstituted polyenes has been experimentally demonstrated.[40] The B3LYP/6-31G** geometry optimizations performed for compounds **1a**−**c** indicate that BLA amounts nearly the same negative value for the three compounds (ca. −0.064 Å), and these results are therefore consistent with the observed positive β values. Thus, the trend of variation of β along the series of compounds studied in this work seems to be mainly determined by the quadratic dependence on L.

Second-Order Nonlinear Optical Properties. The $\mu\beta$ values of compounds **1**−**4** measured using the EFISH technique are gathered in Table 2 along with the $\mu\beta(0)$ values calculated assuming a two-level model (compounds **1a** and **4a** were not measured due to their instability under the EFISH conditions). In comparison, the relevant application parameter $\mu\beta(0)$ for the classical NLO dye DR1 is ca. 600×10^{-48} esu. It can be seen that the nonlinear optical activity is larger for compounds containing better acceptors and that $\mu\beta$ values increase with increasing the length of the ethylenic spacer.

Thermal stability is also an important criterion for technological applications. These compounds show a good degree of thermal stability as evidenced by the decomposition temperatures of compounds **2a** (194 °C), **2b** (195 °C), and **2c** (206 °C).

To gain further understanding of the NLO behavior of these compounds, we have performed theoretical calculations[41] starting with the Finite Field (FF) PM3[42] method,

(37) Del Zoppo, M.; Castiglioni, C.; Zuliani, P.; Razelli, A.; Tommasini, M.; Zerbi, G.; Blanchard-Desce, M. *J. Appl. Polym Sci.* **1998**, *70*, 1311.

(38) (a) Hutchinson, M. H.; Sutton, L. E. *J. Chem. Soc.* **1958**, 4382. (b) Dulcic, A.; Flytzanis, C.; Tang, C. L.; Pépin, D.; Fétizon, M.; Hoppilliard, Y. *J. Chem. Phys.* **1981**, *74*, 1559.

(39) Ortiz, R.; Marder, S. R.; Cheng, L.; Tiemann, B. G.; Cavagnero, S.; Ziller, J. W. *Chem. Commun.* **1994**, 2263.

(40) Bourhill, G.; Brédas, J.-L.; Cheng, L.-T.; Marder, S. R.; Meyers, F.; Perry, J. W.; Tiemann, B. G. *J. Am. Chem. Soc.* **1994**, *116*, 2619.

(41) For reviews on the calculation of second-order nonlinearities using quantum chemical methods, see: (a) Kanis, D. R.; Ratner, M. A.; Marks, T. J. *Chem. Rev.* **1994**, *94*, 195. (b) Morley, J. O.; Pugh, D. In *Nonlinear Optics of Organic Molecules and Polymers*; Nalwa, H. S., Miyata, S., Eds.; CRC: Boca Raton, 1997; p 29.

Table 3. Experimental and Calculated NLO Properties[a] of Compounds 1−4

	exp	FF-PM3			HF/6-31G*//HF/6-31G*			HF/6-31+G*//HF/6-31G*			HF/6-31G*//B3P86/6-31G*		
	$\mu\beta(0)$	m	β_{tot}	$\mu\beta(0)$	m	β_{tot}	$\mu\beta(0)$	m	β_{tot}	$\mu\beta(0)$	m	β_{tot}	$\mu\beta(0)$
1a		4.68	25	109	7.16	15	95	7.34	16	102	7.73	19	129
1b	234[b]	5.00	42	177	7.66	30	202	7.91	32	225	8.63	42	320
1c	320[b]	5.17	59	266	8.25	49	367	8.51	53	410	9.63	78	680
2a	180[c]	5.29	37	167	5.60	16	76	5.62	19	91	6.03	24	120
2b	347[c]	6.19	64	334	6.67	36	214	6.73	41	252	7.60	59	386
2c	455[c]	6.55	92	537	7.42	59	411	7.52	68	476	8.76	96	777
3b (*Z*)	295[d]	5.90	47	104	7.01	35	76	7.12	39	83	7.77	53	150
3b (*E*)		6.70	35	232	8.72	23	189	8.94	25	212	9.87	33	316
3c (*Z*)	611[d]	6.13	64	172	7.45	53	159	7.44	59	210	8.47	92	367
3c (*E*)		6.80	52	351	8.91	39	333	9.12	43	370	10.30	66	659
4b	259[d]	3.63	63	96	5.23	59	165	5.31	64	193	6.06	93	396
4c	570[d]	3.52	81	106	5.22	87	262	5.32	95	304	6.40	153	746

[a] Dipole moments in debye, hyperpolarizabilities in (10^{-30} esu) and $\mu\beta$ in (10^{-48} esu). [b] Measured in chloroform at 1907 nm. [c] Measured in DMSO at 1907 nm. [d] Measured in dichloromethane at 1907 nm.

which has proved to be very accurate in the prediction of the NLO properties of TTF-derived chromophores at a minimal computational cost.[43] These calculations predicted the s-cis conformation of the bond linking the TTF core to the ethylenic spacer as the most stable one, and the FF procedure afforded the results gathered in Table 3. It can be seen that FF-PM3 provides an adequate description of the NLO properties of compounds **1** and **2** but underestimates largely the activity of compounds **3** and **4**. It is noteworthy that in the case of compounds **3**, the less stable *E* isomers are predicted to display larger $\mu\beta$ values.

In an attempt to obtain a better agreement between the observed and calculated $\mu\beta(0)$ values, we have performed ab initio calculations using the coupled perturbed Hartree−Fock (CPHF) method and the medium-size 6-31G* basis set.[44] Although ab initio calculations differ from PM3 in the prediction of the s-trans conformation of the bond linking the TTF moiety to the ethylenic spacer, the calculated $\mu\beta(0)$ values displayed in Table 3 are analogous to FF-PM3 ones and are unable to explain the NLO response of compounds **3** and **4**. Furthermore, while it has been reported that diffuse functions are necessary to obtain accurate hyperpolarizabilities,[45] the use of the 6-31+G* basis set incorporating diffuse functions on heavy atoms causes the prediction of increased $\mu\beta(0)$ values but does not modify the predicted trends in NLO activity (Table 3).

A possible explanation to poor property prediction displayed by semiempirical and Hartree−Fock methods can be found in the used ground-state geometries that are a consequence of the low charge transfer predicted by these methods. Thus, the calculated bond lengths in the ethylenic spacers are 1.45−1.46 Å for single C−C bonds and 1.33−1.34 Å for double C=C bonds, being nearly identical to those of unsubstituted polyenes and corresponding to a bond length alternation[30b,46] (BLA) of 0.11 Å, which should be related to a poor charge transfer in the ground state and a small β value. To obtain better molecular geometries, we have performed optimizations using the B3P86[47]/6-31G* model chemistry that has been

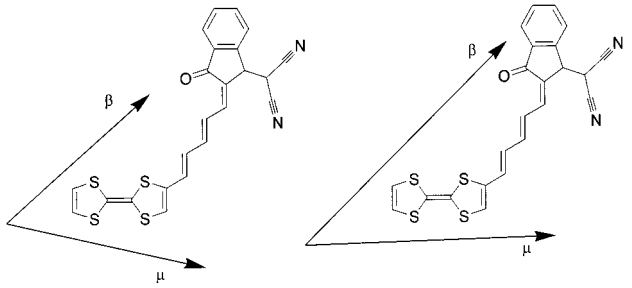

Figure 6. Hyperpolarizability and dipole moment vectors calculated using the HF/6-31G* (left) and B3P86/6-31G* (right) geometries of compound **4c**.

successfully applied to TTF derivatives[48] and provides better C−S bond lengths than the commonly used B3LYP functional.[49] The geometries calculated in this way display distances of 1.42−1.43 and 1.36−1.37 Å for single and double C−C bonds, respectively, corresponding to a BLA of ca. 0.06 Å that is near the optimum value in the search for large hyperpolarizabilities. Unfortunately, DFT methods are unable to predict accurately hyperpolarizabilities due to an incomplete screening of the external electric field,[50] and consequently, we decided to calculate HF hyperpolarizabilities on DFT geometries.

The effect of the geometry on the calculated $\mu\beta(0)$ values of **4c** is depicted in Figure 6. The DFT geometry gives rise to enhanced μ and β values and causes a redirection of the μ vector due to the increased charge transfer from TTF to the acceptor moiety in the ground state.

The $\mu\beta(0)$ values calculated using HF/6-31G*//B3P86/6-31G* are gathered in Table 3, it can be seen that while most of them are somewhat overestimated with respect to the experimental values, this model chemistry yields the best correlation of all the described calculations.

The results obtained for compounds **3** must be commented on separately. While all the theoretical methods

(42) (a) Stewart, J. J. P. *J. Comput. Chem.*, **1989**, *10*, 209. (b) Stewart, J. J. P. *J. Comput. Chem.* **1989**, *10*, 221.
(43) Garín, J.; Orduna, J.; Andreu, R. *Synth. Met.* **1999**, *102*, 1531.
(44) Hariharan, P. C.; Pople, J. A. *Chem. Phys. Lett.* **1972**, *16*, 217.
(45) André, J.-M.; Delhalle, J. *Chem. Rev.* **1991**, *91*, 843.
(46) (a) Marder, S. R.; Cheng, L.-T.; Tiemann, B. G.; Friedli, A. C.; Blanchard-Desce, M.; Perry, J. W.; Skindhøj, J. *Science* **1994**, *263*, 511. (b) Marder, S. R.; Gorman, C. B.; Meyers, F.; Perry, J. W.; Bouhill, G.; Brédas, J.-L.; Pierce, B. M. *Science* **1994**, *265*, 632.
(47) The B3P86 functional consists of Becke's three parameter hybrid functional with the nonlocal correlation provided by Perdew: J. P. Perdew, *Phys. Rev. B* **1986**, *33*, 8822.
(48) (a) Terkia-Derdra, N.; Andreu, R.; Sallé, M.; Levillain, E.; Orduna, J.; Garín, J.; Ortí, E.; Viruela, R.; Pou-Amerigo, R.; Sahraoui, B.; Gorgues, A.; Favard, J.-F.; Riou, A. *Chem. Eur. J.* **2000**, *6*, 1199. (b) Viruela, R.; Viruela, P. M.; Pou-Amerigo, R.; Ortí, E. *Synth. Met.* **1999**, *103*, 1991.
(49) Ma, B.; Lii, J.-H.; Schaefer, H. F., III; Allinger, N. L. *J. Phys. Chem.* **1996**, *100*, 8763.
(50) Champagne, B.; Perpète, E. A.; Jacquemin, D.; Van Gisbergen, S. J. A.; Baerends, E.-J.; Soubra-Ghaoui, C.; Robins, K. A.; Kirtman, B. *J. Phys. Chem.* **2000**, *104*, 4755.

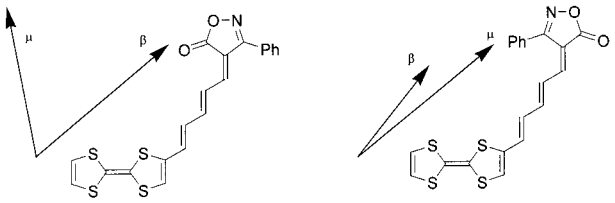

Figure 7. Hyperpolarizability and dipole moment vectors calculated using the HF/6-31G*//B3P86/6-31G* model chemistry for the *Z* and *E* isomers of compound **3c**.

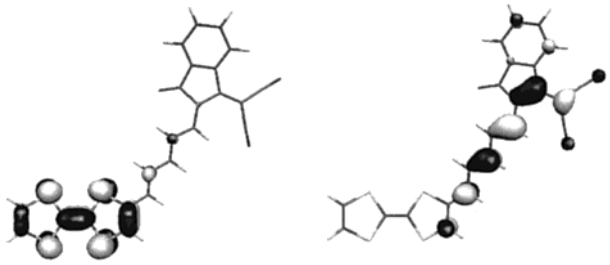

Figure 8. HOMO (−5.65 eV, left) and LUMO (−3.97 eV, right) of compound **4c** calculated by B3P86/6-31G*.

used predict a slightly higher stability of the *Z* isomers compared to the *E* ones, the high electric field used in the EFISH experiments is expected to render the *E* isomers more stable due to their larger dipole moments, and it is feasible that the *E* isomers are responsible for the measured $\mu\beta$ values due to an isomerization under the experimental conditions. This surprising behavior is analogous to the preference for the conformer of higher dipole moment observed on some azo dyes under the EFISH conditions.[51]

The differences in the NLO behavior of the *E* and *Z* isomers of compounds **3** are displayed in Figure 7. It can be seen that while the β_{tot} value calculated for **3c** (*E*) is smaller than that of the *Z* isomer, the better alignement of the μ and β vectors renders the former more active in the EFISH measurements.

The topologies and energies of molecular orbitals have been studied by means of the B3P86/6-31G* model chemistry. The HOMO−LUMO energy gaps calculated in this way, from 1.68 to 2.20 eV, account for this transition as being responsible for the lowest energy absorption in every case. Furthermore, a recent TD-DFT study on compounds **2a**−**c** correctly reproduces the hypsochromic effect observed on lengthening the ethylenic spacer.[52] The charge-transfer character of the HOMO−LUMO transition is demonstrated by the topology of these orbitals (see Figure 8).

The HOMO is analogous to the HOMO of most TTF derivatives and is located mainly on the TTF moiety, while the LUMO extends from the acceptor to the nearest atoms of TTF across the ethylenic spacer. These orbital topologies show the HOMO−LUMO overlap that is a prerequisite[41a] to increase the allowedness of the charge transfer transition and consequently the nonlinear optical response.

Summary and Conclusions

In summary, we describe the synthesis of novel TTF-based π-conjugated donor−acceptor systems (**1**−**4**) in which the donor TTF unit is connected to different acceptor moieties through an oligoenic spacer of variable length. The CV measurements reveal an amphoteric behavior showing two reversible oxidation waves corresponding to the formation of the radical cation and dication species of the TTF moiety and an irreversible reduction wave corresponding to the electron-accepting moiety.

The barbituric acid derivatives (**2a**−**c**) showed stronger electron-acceptor properties than the remaining acceptors, as judged from their reduction potential values.

All the D-π-A systems showed an intramolecular charge transfer band in their electronic spectra which is strongly influenced by the acceptor ability of the acceptor moiety as well as by the length of the oligoenic spacer. Thus, a red shift of the lowest energy absorption band was observed when increasing the acceptor strength. However, a most interesting observation was the hypsochromic shift when increasing the length of the oligoenic spacer. This fact, which at present has not a clear explanation, has been analyzed by UV−vis and Raman spectroscopy. In particular, we have found that the characteristic Raman-active ν_3 mode associated to the TTF moiety (identified on the basis of B3LYP/6-31G** force field quantum chemical calculations) undergoes an upshift with increasing length of the π-spacer, thus suggesting a less effective intramolecular charge transfer as derived from previous empirical relations.

All the studied compounds (**1**−**4**) showed high second-order NLO responses that were measured by using the EFISH technique. The higher $\mu\beta$ values were obtained for those TTF derivatives bearing the stronger acceptors and larger oligoenic spacers.

Theoretical calculations carried out at the semiempirical (FF-PM3) and ab initio (HF/6-31G* and HF/6-31+G*) levels reveal a good agreement with the $\mu\beta(0)$ experimental values, although these values were somewhat overestimated when HF/6-31G*//B3P86/6-31G* was used.

The topologies and energies of molecular orbitals were studied by B3P86/6-31G* showing that the HOMO−LUMO energy gaps account for the observed intramolecular charge transfer from the donor TTF to the LUMO, which is mainly located on the acceptor moiety.

Work is currently in progress directed to the preparation of other TTF derivatives exhibiting NLO properties which throw some light on the most unusual observed hypsochromic shifts in these TTF-π-A compounds when increasing the conjugation of the π-system.

Experimental Section

All melting points were measured with a Gallenkamp apparatus and are uncorrected. IR spectra were recorded either as KBr pellets or as films with NaCl plates with a Perkin-Elmer 257 spectrometer. UV−vis spectra were recorded with a Perkin-Elmer Lambda 3 instrument. ^{13}C and ^{1}H NMR spectra were recorded with a Varian VXR-300 spectrometer (300 and 75 MHz for ^{1}H and ^{13}C, respectively; chemical shifts are given as δ values (int. Standard: TMS). Fourier Transform Infrared absorption (FT-IR) measurements were made with a Perkin-Elmer Model 1760 X spectrometer. All spectra were collected using a resolution of 2 cm^{-1}, and the mean of 50 scans was obtained. Interference from atmospheric water vapor was minimized by purging the instrument for 10−15 min with dry argon before beginning data collection. Fourier transform Raman (FT-Raman) spectra were recorded using a Bruker FRA106/S apparatus with a germanium photoresistor operating at liquid nitrogen temperatures as the near-infrared

(51) Morley, J. O.; Hutchings, M. G.; Zyss, J.; Ledoux, I. *J. Chem. Soc., Perkin Trans. 2* **1997**, 1139.

(52) Andreu, R.; Garín, J.; Orduna, J. *Tetrahedron* **2001**, *57*, 7883.

detector. Radiation of 1064 nm from a Nd:YAG laser was used for Raman excitation with the operating power adjusted to 100 mW. Light reflected and scattered off the samples was filtered to remove that elastically scattered and then passed through a Michelson interferometer in a backscattering arrangement. Samples were analyzed as pure solids in sealed capillaries. One thousand scans were added to increase the signal-to-noise ratio. Spectra were plotted after baseline correction to remove the fluorescence showed by the samples in the near-infrared region. Elemental analyses were performed with a Perkin-Elmer CHN 2400 apparatus. MS were recorded with a Hewlet-Packard HP5989A spectrometer. EFISH measurements were taken with a nonlinear optics spectrometer from SOPRA. The fundamental light at 1.907 μm was the first Stokes peak of a hydrogen Raman cell pumped by the 1.064 μm light from a Q-switched Nd:YAG laser (Quantel YG 781, 10 pps, 8 ns, pulse). That light was passed through a linear polarizer and focused on the EFISH cell. The polarizing dc voltage (parallel to the light polarization) used in this cell was 6 kV. The output light from the cell was passed through an interference filter to select the second harmonic light (0.954 μm), which was finally detected with a R642 photomultiplier from Hamamatsu. Static $\mu\beta(0)$ values were deduced from the experimental values using a two-level dispersion model. Cyclic voltammograms were recorded on a potentiostat/galvanostat Versastat EG & G PAR, equipped with a software electrochemical analysis Model 250 by using a GCE (glassy carbon) as working electrode, SCE as reference electrode, $Bu_4N^+ClO_4$ as supporting electrolyte, dichloromethane as solvent, and at a scan rate of 200 mV/s. Tetrathiafulvalene (TTF), *N*,*N*-dimethylaminoacroleine, *N*,*N*-diethylthiobarbituric acid, 3-phenyl-5-isoxazolone and 1,3-indandione are commercially available and were used without further purification. Ethanol and tetrahydrofuran were dried with sodium and were distilled before use. Theoretical calculations were performed with the Gaussian 94 and Gaussian 98[53] programs. Geometry optimizations were performed on isolated entities using the default convergence criteria, and harmonic vibrational frequencies and molecular hyperpolarizabilities were calculated analytically using the CPHF procedure. Semiempirical FF-PM3 calculations were performed using MOPAC 6.0.[54]

(*E*)-3-(Tetrathiafulvalenyl)acrylaldehyde (5b). Under argon atmosphere, at −78 °C, 0.73 mL (1.09 mmol) of a 1.5 M solution of lithium diisopropylamide (LDA) in tetrahydrofuran/heptane was added to a solution of 204 mg (1 mmol) of TTF in 10 mL of dry THF. Then, 99 mg (1 mmol) of 3-(dimethylamino)-acrolein (**7**) was added and the reaction was allowed to reach room temperature overnight. Afterward, the mixture was poured over a 2 M aqueous solution of hydrochloric acid. The organic layer was extracted with diethyl ether and dried over sodium sulfate. After vacuum elimination of the solvent, the residue obtained was chromatographed (hexane/dichloromethane) to yield 155 mg (60%) of **5b** as a red solid: mp 121−122 °C (lit.[25] mp 121−122 °C).

5-(Tetrathiafulvalenyl)penta-2,4-dien-1-al (5c). Under argon atmosphere, at −78 °C, 0.73 mL (1.09 mmol) of a 1.5 M solution of lithium diisopropylamide (LDA) in tetrahydrofuran/heptane was added to a solution of 204 mg (1 mmol) of TTF in 10 mL of dry THF. Then, 125 mg (1 mmol) of 5-(*N*,*N*-diethylamino)-2,4-pentadienal[27] (**8**) was added, and the reaction was allowed to reach room temperature overnight. Afterward, the mixture was poured over a 2 M aqueous solution of hydrochloric acid. The organic layer was extracted with diethyl ether and dried over sodium sulfate. After vacuum elimination of the solvent, the residue obtained was chromatographed (hexane/dichloromethane) to yield 91 mg (32%) of **5b** as a red solid: mp 151−152 °C; ^{1}H NMR ($CDCl_3$, 300 MHz) δ 9.59 (d, J = 7.8 Hz, 1H), 7.12 (dd, J = 15.3, 11.4 Hz, 1H), 6.75 (d, J = 15.3 Hz, 1H), 6.61 (s, 1H), 6.35 (s, 2H), 6.27 (dd, J = 14.7, 11.4 Hz, 1H), 6.22 (dd, J = 14.7, 7.8 Hz, 1H); ^{13}C NMR ($CDCl_3$, 75 MHz) δ 193.1, 150.4, 135.2, 132.3, 131.9, 128.7, 125.1, 119.1, 118.9, 114.1, 106.1; FTIR (KBr, cm^{-1}) 1660, 1605, 1582, 1504, 114, 1160; UV−vis (CH_2Cl_2) λ_{max} (nm) 520, 334; MS *m*/*z* (rel intensity) 284 (M^+, 100). Anal. Calcd for $C_{11}H_8OS_4$: C, 46.49; H, 2.84. Found: C, 46.82; H, 2.97.

2-(6,6-Dicyanohexatrienyl)tetrathiafulvalene (1c). A solution of 227 mg (0.8 mmol) of 5-(tetrathiafulvalenyl)penta-2,4-dienal (**5c**), 244 mg (3.30 mmol) of malononitrile, 0.18 mL of ammonium acetate, and 0.18 mL of acetic acid in 25 mL of toluene was refluxed, under azeotropic removal of water, for 24 h. The solvent was evaporated, and the crude product was purified by flash chromatography by using hexane/methylene chloride as the eluent to afford 160 mg (60%) of **1c** as a red solid: mp 201−202 °C; ^{1}H NMR (DMSO-d_6, 300 MHz) δ 8.14 (d, J = 11.2 Hz, 1H), 7.29 (s, 1H), 7.24 (dd, J = 13.7, 12.7 Hz, 1H), 7.08 (d, J = 13.7 Hz, 1H), 6.93 (dd, J = 12.7, 12.7 Hz, 1H), 6.75 (s, 2H), 6.51 (dd, J = 12.7, 11.2 Hz, 1H); ^{13}C NMR (DMSO-d_6, 75 MHz) δ 161.07, 150.50, 148.29, 144.12, 135.13, 133.69, 129.99, 128.79, 127.48, 120.17, 114.71, 114.50, 112.67, 112.47; FTIR (KBr, cm^{-1}) 2230, 2219, 1584, 1538, 1496, 1363, 1287, 1153; UV−vis (CH_2Cl_2) λ_{max} (nm) 608, 392; MS *m*/*z* (rel intensity) 332 (M^+, 100). Anal. Calcd for $C_{14}H_8N_2S_4$: C, 50.61; H, 2.40; N, 8.44. Found: C, 51.02; H, 2.57; N, 8.79.

Synthesis of TTF Derivatives 2a−c. General Procedure. A 200 mg (1 mmol) sample of diethylthiobarbituric acid (**9**) was added to a solution of 1 mmol of the corresponding formyl-TTF derivative (**5a**−**c**) in 15 mL of dry ethanol. The solution was refluxed under argon atmosphere with exclusion of light for 2 h. After this time, the precipitated solid was filtered, washed thoroughly with ethanol, and purified by flash chromatography (hexane/dichloromethane) to afford derivatives **2a**−**c** as red solids.

1,3-Diethyl-5-(tetrathiafulvalenylmethylidene)-2-thiobarbituric Acid (2a). By following the above general procedure and using formyl-TTF (**5a**) as the reagent, derivative **2a** was obtained in a 67% yield: mp 215−216 °C; ^{1}H NMR (DMSO-d_6, 300 MHz) δ 7.93 (s, 1H), 7.66 (s, 1H), 6.35 (m, 2H), 4.51 (m, 4H), 1.28 (m, 6H); FTIR (KBr, cm^{-1}) 3042, 2975, 2928, 1685, 1652, 1541, 1379, 1363, 1097; UV−vis (CH_2Cl_2) λ_{max} (nm) 718, 384, 316, 266; MS. *m*/*z* (rel intensity) 414 (M^+, 100). Anal. Calcd for $C_{15}H_{14}N_2O_2S_5$: C, 43.46; H, 3.40; N, 6.76. Found: C, 43.99; H, 3.21; N, 7.28.

1,3-Diethyl-5-(3-tetrathiafulvalenyl-2-propenylidene)-2-thiobarbituric Acid (2b). By following the above general procedure and using (*E*)-3-(tetrathiafulvalenyl)acrylaldehyde (**5b**) as the reagent, derivative **2b** was obtained in a 65% yield: mp 205−206 °C; ^{1}H NMR (DMSO-d_6, 300 MHz) δ 8.03 (d, J = 12.7 Hz, 1H), 7.75 (dd, J = 14.1 Hz, J' = 11.7 Hz, 1H), 7.10 (d, J = 14.7 Hz, 1H), 6.96 (s, 1H), 6.35 (m, 2H), 4.52 (m, 4H), 1.27 (m, 6H); FTIR (KBr, cm^{-1}) 3057, 2966, 2924, 1652, 1544, 1449, 1386, 1079; UV−vis (CH_2Cl_2) λ_{max} (nm) 672, 404, 312. Anal. Calcd for $C_{17}H_{16}N_2O_2S_5$: C, 46.37; H, 3.66; N, 6.37. Found: C, 46.88; H, 4.09; N, 6.79.

1,3-Diethyl-5-(5-tetrathiafulvalenyl-2,4-pentadienylidene)-2-thiobarbituric Acid (2c). By following the above general procedure and using 5-(tetrathiafulvalenyl)penta-2,4-dienal (**5c**) as the reagent, derivative **2c** was obtained in a 58% yield: mp 199−200 °C; ^{1}H NMR (DMSO-d_6, 300 MHz) δ 8.07 (d, J = 12.9 Hz, 1H), 7.70 (m, 1H), 7.54 (m, 1H), 7.12 (m, 1H), 6.78 (d, J = 14.1 Hz, 1H), 6.68 (s, 1H), 6.33 (m, 2H), 4.53 (m, 4H), 1.29 (m, 6H); FTIR (KBr, cm^{-1}) 2977, 2928, 2854, 1686, 1575, 1521, 1493, 1376; UV−vis (CH_2Cl_2) λ_{max} (nm) 648, 430, 310; MS *m*/*z* (rel intensity) 466 (M^+, 100). Anal. Calcd for $C_{19}H_{18}N_2O_2S_5$: C, 48.93; H, 3.89; N, 6.01. Found: C, 48.79; H, 3.77; N, 6.45.

(53) Gaussian 98, Revision A.7: Frisch, M. J.; Trucks, G. W.; Schlegel, H. B.; Scuseria, G. E.; Robb, M. A.; Cheeseman, J. R.; Zakrzewski, V. G.; Montgomery, J. A., Jr.; Stratmann, R. E.; Burant, J. C.; Dapprich, S.; Millam, J. M.; Daniels, A. D.; Kudin, K. N.; Strain, M. C.; Farkas, O.; Tomasi, J.; Barone, V.; Cossi, M.; Cammi, R.; Mennucci, B.; Pomelli, C.; Adamo, C.; Clifford, S.; Ochterski, J.; Petersson, G. A.; Ayala, P. Y.; Cui, Q.; Morokuma, K.; Malick, D. K.; Rabuck, A. D.; Raghavachari, K.; Foresman, J. B.; Cioslowski, J.; Ortiz, J. V.; Baboul, A. G.; Stefanov, B. B.; Liu, G.; Liashenko, A.; Piskorz, P.; Komaromi, I.; Gomperts, R.; Martin, R. L.; Fox, D. J.; Keith, T.; Al-Laham, M. A.; Peng, C. Y.; Nanayakkara, A.; Gonzalez, C.; Challacombe, M.; Gill, P. M. W.; Johnson, B.; Chen, W.; Wong, M. W.; Andres, J. L.; Gonzalez, C.; Head-Gordon, M.; Replogle, E. S.; Pople, J. A. Gaussian, Inc., Pittsburgh, PA, 1998.

(54) MOPAC 6.0: J. J. P. Stewart, QCPE, **1990**, *10*, 455.

Synthesis of TTF Derivatives 3b,c. General Procedure. A 161 mg (1 mmol) sample of 3-phenyl-5-isoxazolone (**10**) was added to a solution of 1 mmol of the corresponding formyl-TTF derivative (**5a**−**c**) in 15 mL of dry ethanol. The solution was refluxed under argon atmosphere with exclusion of light for 2 h. After this time, the precipitated solid was filtered, washed thoroughly with ethanol, and purified by flash chromatography (hexane/dichloromethane) to afford derivatives **3b**,**c** as red solids.

3-Phenyl-4-(3-tetrathiafulvalenyl-2-propenyliden)-5-isoxazolone (3b). By following the above general procedure and using (*E*)-3-(tetrathiafulvalenyl)acrylaldehyde (**5b**) as the reagent, derivative **3b** was obtained in a 72% yield: mp 214−216 °C; ^{1}H NMR (DMSO-d_6, 300 MHz) δ 7.72 (d, J = 14.7 Hz, 1H), 7.68−7.57 (m, 5H), 7.35 (s, 1H), 7.29 (d, J = 14.4 Hz, 1H), 6. 79 (m, 2H), 5.90 (dd, J = 14.7 Hz, J' = 11.7 Hz, 1H); ^{13}C NMR (DMSO-d_6, 75 MHz) δ 169.1, 164.9, 161.9, 149.9, 141.7, 135.7, 135.0, 131.0, 129.2, 128.5, 128.2, 127.1, 123.8, 120.3, 120.1, 115.9, 114.8, 104.8; FTIR (KBr, cm^{-1}) 3066, 1750, 1606, 1574, 1523, 1490, 1385, 1196, 1165, 1104; UV−vis (CH_2Cl_2) λ_{max} (nm) 658, 382, 320; MS *m*/*z* (rel intensity) 01 (M^+, 100). Anal. Calcd for $C_{18}H_{11}NO_2S_4$: C, 53.87; H, 2.76; N, 3.49. Found: C, 54.46; H, 3.12; N, 3.89.

3-Phenyl-4-(5-tetrathiafulvalenyl-2,4-pentadienyliden)-5-isoxazolone (3c). By following the above general procedure and using 5-(tetrathiafulvalenyl)penta-2,4-dienal (**5c**) as the reagent, derivative **3c** was obtained in a 69% yield: mp 207−209 °C dec; ^{1}H NMR (DMSO-d_6, 300 MHz) δ 7.81 (dd, J = 13.8 Hz, J' = 11.5 Hz, 1H), 7.79 (d, J = 14.7 Hz, 1H), 7.70−7.57 (m, 5H), 7.45 (dd, J = 15.1 Hz, J' = 10.8 Hz, 1H), 7.36 (s, 1H), 7.04 (d, J = 14.7 Hz, 1H), 6.77 (s, 2H), 6.52 (dd, J = 15.3 Hz, J' = 11.4 Hz, 1 H); ^{13}C NMR (DMSO-d_6, 75 MHz) δ 169.0, 164.9, 163.4, 162.3, 153.3, 150.5, 147.7, 135.4, 133.5, 131.0, 130.8, 129.3, 129.2, 128.3, 127.6, 127.3, 120.3, 120.1, 114.0, 106.1; UV−vis (CH_2Cl_2) λ_{max} (nm) 630, 408, 320; MS *m*/*z* (rel intensity) 427 (M^+, 100). Anal. Calcd for $C_{20}H_{13}NO_2S_4$: C, 56.21; H, 3.07; N, 3.28. Found: C, 55.99; H, 3.26; N, 3.79.

Synthesis of TTF Derivatives 4a−c. General Procedure. A 194 mg (1 mmol) sample of dicyanomethyleneindandione (**11**)[9] was added to a solution of 1 mmol of the corresponding formyl-TTF derivative (**5a**−**c**) in 15 mL of acetic anhydride. The solution was refluxed under argon atmosphere with exclusion of light for 2 h. After this time, the precipitated solid was filtered, washed thoroughly with ethanol, and purified by flash chromatography (hexane/dichloromethane) to afford derivatives **4a**−**c** as red solids.

3-Dicyanomethylen-2-(tetrathiafulvalenylmethyliden)-1-indanone (4a). By following the above general procedure and using formyl-TTF (**5a**) as the reagent, derivative **4a** was obtained in a 52% yield: mp > 300 °C; ^{1}H NMR (DMSO-d_6, 300 MHz) δ 8.69 (d, 1H), 8.22 (s, 1H), 7.93 (d, 1H), 7.78 (m, 2H), 7.66 (s, 1H), 6.41 (d, 1H), 6.36 (d, 1H); ^{13}C NMR (DMSO-d_6, 75 MHz) δ 176.3, 169.6, 147.1, 135.5, 131.2, 129.4, 127.1, 123.8, 121.3, 120.7, 113.7, 110.8, 109.5, 108.5, 107.9, 106.8, 104.7, 104.5, 103.2; FTIR (KBr, cm^{-1}) 2214, 1701, 1589, 1541, 1471, 1456, 1375, 1342; UV−vis (CH_2Cl_2) λ_{max} (nm) 798, 390, 310, 230. Anal. Calcd for $C_{19}H_8N_2OS_4$: C, 55.89; H, 1.98; N, 6.87. Found: C, 56.49; H, 2.24; N, 7.51.

3-Dicyanomethylen-2-(3-tetrathiafulvalenyl-2-propenyliden)-1-indanone (4b). By following the above general procedure and using (*E*)-3-(tetrathiafulvalenyl)acrylaldehyde (**5b**) as the reagent, derivative **4b** was obtained in a 47% yield: mp > 300 °C; ^{1}H NMR (DMSO-d_6, 300 MHz) δ 8.51 (d, 1H), 8.19 (d, 1H), 7.96 (m, 2H), 7.89 (d, 1H), 7.78 (m, 1H), 7.74 (s, 1H), 7.55 (d, 1H), 6.80 (s, 2H); FTIR (KBr, cm^{-1}) 2218, 1697, 1591, 1569, 1541, 1481, 1456, 1359, 1342; UV−vis (CH_2Cl_2) λ_{max} (nm) 726, 428, 308, 218 Anal. Calcd for $C_{21}H_{10}N_2OS_4$: C, 58.07; H, 2.32; N, 6.45. Found: C, 58.62; H, 2.59; N, 7.02.

3-Dicyanomethylen-2-(5-tetrathiafulvalenyl-2,4-pentadienyliden)-1-indanone (4c). By following the above general procedure and using 5-(tetrathiafulvalenyl)penta-2,4-dienal (5**c**) as the reagent, derivative **4c** was obtained in a 45% yield: mp > 300 °C; FTIR (KBr, cm^{-1}) 2212, 1697, 1575, 1522, 1483, 1458, 1379, 1340; UV−vis (CH_2Cl_2) λ_{max} (nm) 690, 458, 300, 222; MS *m*/*z* (rel intensity) 466 (M^+, 100). Anal. Calcd for $C_{23}H_{12}N_2OS_4$: C, 60.00; H, 2.63; N, 6.09. Found: C, 60.55; H, 3.22; N, 6.71.

Acknowledgment. This work has been partially supported by the DGESIC of Spain (Projects PB98-0818, BQU2000-0790, MAT99-1009-C02-02, FD97-1765-C03, and BQU2000-1156).

Supporting Information Available: B3P86/6-31G* geometries (Cartesian coordinates) and energies (atomic units) of compounds **1a**−**c**, **2a**−**c**, **3b**,**c**, and **4b**,**c**. This material is available free of charge via the Internet at http://pubs.acs.org.

JO010717K